Astron. Astrophys. 354, 567–572 (2000)

ASTRONOMY AND ASTROPHYSICS

*Rossi*XTE and *Beppo*SAX observations of the Be/neutron star system RX J0146.9+6121

S. Mereghetti[1], **A. Tiengo**[1,2], **G.L. Israel**[3,⋆], **and L. Stella**[3,⋆]

[1] Istituto di Fisica Cosmica "G.Occhialini", Via Bassini 15, 20133 Milano, Italy
[2] Dipartimento di Fisica, Università di Milano, Via Celoria 16, 20133 Milano, Italy
[3] Osservatorio Astronomico di Roma, Via dell'Osservatorio 2, 00040 Monteporzio Catone (Roma), Italy

Received 19 July 1999 / Accepted 2 December 1999

Abstract. We report *Rossi*XTE and *Beppo*SAX observations of the X–ray pulsar RX J0146.9+6121, the neutron star/Be binary system with the longest known spin period.

Data obtained one month after the most recent outburst (July 1997), show that the source has returned to its normal luminosity of a few 10^{34} erg s^{-1} while spin-up continued at an average rate of $\sim 5 \times 10^{-8}$ s s^{-1}.

Key words: stars: individual: RX J0146.9+6121 – X-rays: stars

1. Introduction

RX J0146.9+6121 is an accreting neutron star with a ∼25 min spin period, the longest known period of any X-ray pulsar in a Be-star system. This fact was realized (Mereghetti et al. 1993) only after the re–discovery of this source in the ROSAT All Sky Survey and its identification with the 11^{th} magnitude Be star LS I +61° 235 (Motch et al. 1991). Indeed the 25 min periodicity had already been discovered with EXOSAT (White et al. 1987), but it was attributed to a nearby source (4U 0142+614; see also Israel et al. 1994, Hellier 1994).

The optical companion of RX J0146.9+6121 was classified as B5IIIe (Slettebak 1985), but Coe et al. (1993) derived a somewhat earlier spectral type of O9–B0. This star is probably a member of the open cluster NGC 663 at a distance of about 2.5 kpc (Tapia et al. 1991). For this distance, the 1–20 keV luminosity during the EXOSAT detection in 1984 was $\sim 10^{36}$ erg s^{-1} (Mereghetti et al. 1993).

All the observations of RX J0146.9+6121 carried out after its re-discovery yielded lower luminosities, of the order of a few 10^{34} erg s^{-1} (Hellier 1994; Haberl et al. 1998a), until an observation with the *Rossi*XTE satellite showed that in July 1997 the flux started to rise again (Haberl et al. 1998b), though not up to the level of the first EXOSAT observation.

Here we report on observations performed with the *Rossi*XTE (Bradt et al. 1993) and *Beppo*SAX (Boella et al. 1997a) satellites from 1996 to 1998.

Send offprint requests to: S. Mereghetti (sandro@ifctr.mi.cnr.it)
⋆ Affiliated to I.C.R.A.

2. *Rossi*XTE observations

2.1. Spectral analysis

RX J0146.9+6121 was observed with the *Rossi*XTE satellite on March 28, 1996 from 11:17 UT to 22:11 UT. The results presented here are based on data collected with the Proportional Counter Array (PCA, Jahoda et al. 1996). The PCA instrument consists of an array of 5 proportional counters operating in the 2–60 keV energy range, with a total effective area of approximately 7000 cm^2 and a field of view, defined by passive collimators, of $\sim 1^\circ$ FWHM.

For the analysis of the PCA data, time intervals with a source elevation angle greater than 10° were selected, resulting in a net exposure time of about 18.5 ks. Only the top layer anodes of the five proportional counters were used to accumulate spectra and light curves of RX J0146.9+6121. The background was estimated using the latest version of the program PCABACKEST applicable to the time period of our observation (version 1.5). To account for the uncertainties in the response matrix (version 2.2.1), we added a 2% systematic error to the PHA data.

Attempts to fit the PCA spectrum with single component models gave unacceptable results, due to the presence of some contamination from the nearby source 4U 0142+614. In fact the PCA collimator (Strohmayer & Jahoda 1998) has a transmission of about 58% at the off-axis angle of this pulsar (∼24'). Since the luminosity of 4U 0142+614 shows little or no variability on long timescales (Israel et al. 1999a) we can estimate its contribution and model it in the spectral analysis. Assuming the spectral parameters measured with ASCA (White et al. 1996; $N_H = 0.95 \times 10^{22}$ cm^{-2}, power law photon index α = 3.67, blackbody temperature kT = 0.386 keV) and reducing the normalization according to the collimator response, we expect from 4U 0142+614 ∼10 counts s^{-1} in the 2-20 keV range. This corresponds to about 18% of the background-subtracted counts detected by the PCA in the same energy range. Due to the soft spectrum of 4U 0142+614, its contribution rises to over 35% of the counts in the 2-4 keV range. Therefore we included in the fits the contribution from 4U 0142+614 with spectral parameters fixed at the above values.

Even taking the contribution from 4U 0142+614 into account, a single power law cannot describe the spectrum of RX

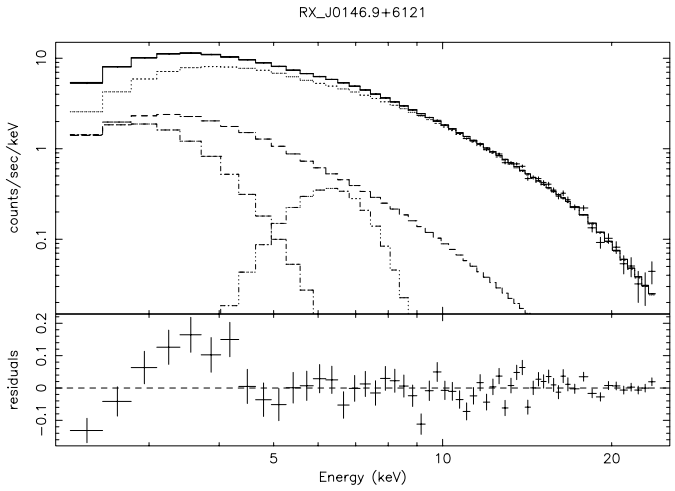

Fig. 1. The *Rossi*XTE PCA best fit spectrum and its different model components, corresponding to the parameters in Table 1. Residuals are shown in the lower panel.

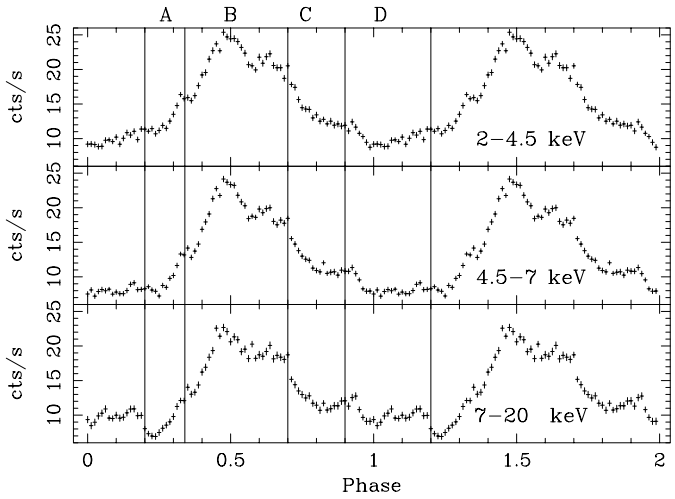

Fig. 2. The *Rossi*XTE PCA light curve of RX J0146.9+6121 folded at its 1407.8 s period, plotted in 3 different ranges of energy. The contribution of the background and of 4U 0142+614 has been subtracted. The vertical lines show the 4 phase intervals chosen for the pulse phase spectroscopy.

Table 1. Results of the *Rossi*XTE PCA spectral analysis. All errors represent 90% confidence limits after introducing the 2% systematic error.

RX J0146.9+6121	photon index	$2.05^{+0.04}_{-0.43}$
	N_H (atoms cm^{-2})	$<2.2\ 10^{22}$
	E_{cutoff} (keV)	17.2 ± 0.9
	E_{fold} (keV)	$7.0^{+4.1}_{-2.5}$
line	E (keV)	$6.3^{+0.4}_{-1.7}$
	σ (keV)	$0.8^{+2.5}_{-0.5}$
	EW (eV)	168
4U 0142+614	N_H (atoms cm^{-2})	$0.95\ 10^{22}$
(fixed	photon index	3.67
parameters)	power law norm	0.09
	blackbody kT	0.386 keV
	blackbody norm	334 km^2/10 kpc^2
χ^2_ν/dof		1.24/50

J0146.9+6121. The residuals show clear evidence for an iron K emission line and for a spectral turnover at energies above ∼15 keV. A better fit can be obtained by adding to the model a Gaussian emission line and an exponential cut-off (or a broken power law). The best fit spectrum is shown in Fig. 1 and its parameters are reported in Table 1.

Since RX J0146.9+6121 lies at low galactic latitude (l=129°.5, b=–0°.8) it is likely that the observed iron line result from the diffuse emission from the galactic ridge (Koyama et al. 1989; Yamauchi & Koyama 1993). Based on the work by Yamauchi & Koyama we derived the flux from the diffuse line emission expected within the field of view of the PCA instrument. Though several uncertainties are involved in this estimate and the parameters of the Fe line reported in Table 1 are affected by the uncertainty in the PCA calibration around the Xenon L edge (at ∼5.5 keV; see, e.g., Fig. 1 in Dove et al. 1998), we find that the observed Fe-line flux can be easily accounted for. This conclusion is further supported by the absence of line emission in the RX J0146.9+6121 spectrum obtained with the ASCA imaging instruments (Haberl et al. 1998b), which allow a better subtraction of the local background.

The flux of RX J0146.9+6121 in the 2-20 keV range corresponding to the best fit parameters is 1.3×10^{-10} erg cm^{-2} s^{-1} (1.4×10^{-10} erg cm^{-2} s^{-1}, corrected for the absorption). For a distance of 2.5 kpc this corresponds to a luminosity of $\sim10^{35}$ erg s^{-1}.

2.2. Timing analysis

To derive the pulse period of RX J0146.9+6121 we used a standard folding technique, obtaining a value of 1407.8 ± 1.3 s. The light curve, shown for three different energy ranges in Fig. 2, has a single broad peak, as seen in previous observations (ASCA, ROSAT, see Haberl et al. 1998b; *Rossi*XTE see Haberl et al. 1998a). Moreover, thanks to the considerably higher signal to noise ratio, some substructures are clearly visible in our data, as well as significant pulse to pulse variability. This is shown in Fig. 3 where we have plotted most of the individual pulses visible in our observation.

2.3. Phase-resolved spectroscopy

Some evidence for spectral variations as a function of the spin period phase are apparent from Fig. 2. To investigate this in more detail, we extracted background subtracted spectra corresponding to the four phase intervals marked in Fig. 2. As a first step, we fitted the total spectrum with the model of Table 1 and then, keeping all other parameters fixed, we renormalized the power law representing RX J0146.9+6121 for each of the four phase intervals; the ratios of the observed spectra to these renormalized average models are shown in Fig. 4. Some features are clearly seen in these plots: (1) a considerable excess above 10

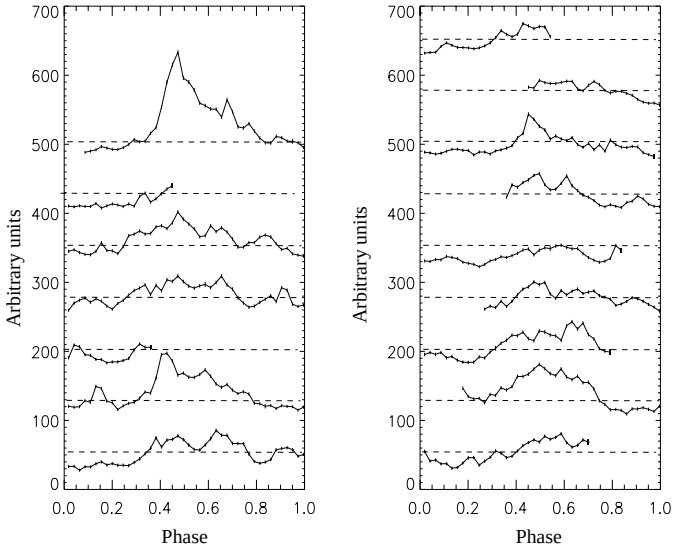

Fig. 3. Light curves of individual pulses of RX J0146.9+6121. The time sequence of the pulses is from bottom-left to top-right. Each pulse has been offset by an arbitrary constant, but the ordinate scale is the same for all the curves. The dashed lines correspond to the average count rate of the whole observation (55 counts s^{-1}).

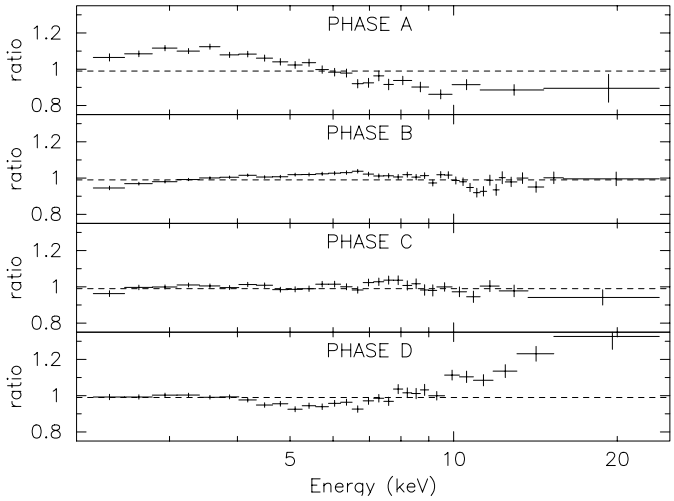

Fig. 4. Ratios of the spectra corresponding to the phase intervals shown in Fig. 2 to the average model spectrum. The model is a power law with low-energy absorption and high-energy cutoff (and the fixed components discussed in the text to account for 4U 0142+614 and the galactic ridge iron line). The parameters are fixed at the best-fit values for the total spectrum, except for the normalization that is the best-fit value for each phase interval.

keV during the interval D, (2) a softening of the whole spectrum during the interval A, (3) a slight variation of the intermediate energy structure with phase.

To investigate which components of the spectrum are phase dependent, the four spectra were fitted with the model discussed above, keeping the parameters corresponding to the 4U 0142+614 contamination and to the Fe-line fixed. The results are reported in Table 2. Significant variations are seen in the power law spectral index and absorption, while the errors in the cut-off parameters are too large to establish a definite variation in the different pulse phase intervals. Note that during phase interval D, we obtain an upper limit to the photoelectric absorption lower than the value expected for RX J0146.9+6121 from optical observations (Motch et al. 1997). This is an indication that the model used is oversimplified and more spectral components are probably required, at least at certain phase intervals.

Table 2. Results of the *Rossi*XTE PCA phase-resolved spectroscopy. All errors represent 90% confidence limits after intoducing the 2% systematic error.

Phase A	phot.index	2.27 ± 0.06
	N_H	$1.4\pm0.5\ 10^{22}$
	E_{cutoff}	$17.6^{+3.9}_{-3.2}$ keV
	E_{fold}	$4.6^{+34.5}_{-4.6}$ keV
	χ^2_ν/dof	0.90/53
Phase B	phot.index	2.14 ± 0.03
	N_H	$2.7^{+0.4}_{-0.3}\ 10^{22}$
	E_{cutoff}	$17.3^{+1.3}_{-1.5}$ keV
	E_{fold}	$8.5^{+8.8}_{-4.1}$ keV
	χ^2_ν/dof	0.81/53
Phase C	phot.index	2.08 ± 0.05
	N_H	$2.1\pm0.4\ 10^{22}$
	E_{cutoff}	$16.6^{+1.9}_{-1.7}$ keV
	E_{fold}	$5.0^{+7.1}_{-3.4}$ keV
	χ^2_ν/dof	0.85/53
Phase D	phot.index	$1.77^{+0.04}_{-0.03}$
	N_H	$< 0.4\ 10^{22}$
	E_{cutoff}	$17.7^{+2.3}_{-2.2}$ keV
	E_{fold}	$7.8^{+19.6}_{-5.1}$ keV
	χ^2_ν/dof	0.93/53

3. *Beppo*SAX observations

We have analyzed the data from the the Low–Energy Concentrator Spectrometer (LECS; 0.1–10 keV; Parmar et al. 1997) and Medium–Energy Concentrator Spectrometer (MECS; 1.3–10 keV; Boella et al. 1997b). The MECS instrument consists of three identical grazing incidence telescopes with imaging gas scintillation proportional counters in their focal planes. The LECS instrument uses an identical concentrator system as the MECS, but utilizes an ultra–thin (1.25 μm) detector entrance window and a driftless configuration to extend the low–energy response to 0.1 keV. The fields of view of the LECS and MECS are circular with diameters of 37′ and 56′ respectively. The energy resolution of both instruments is $\sim 8.5\sqrt{6/E_{keV}}$% FWHM. In the overlapping energy range, the angular resolution of both instruments is similar and corresponds to 90% encircled energy within a radius of 2′.5 at 1.5 keV.

The RX J0146.9+6121 position is included at various offset angles in four *Beppo*SAX observations of 4U 0142+614 (see Table 3). The original project was to monitor RX J0146.9+6121 in order to remove the high energy contribution of this pulsar from that of 4U 0142+614 in the non–imaging instruments. The

Table 3. *Beppo*SAX Observation log

Start Time (UT)	Stop Time (UT)	MECS Exposure Time (s)	Count rate MECS cts/s	Off–axis angle ($'$)
03–Jan–97 05:47:20	04–Jan 02:08:50	48226	0.156±0.002[a]	20
09–Aug–97 23:12:45	10–Aug 07:37:40	16757	0.132±0.003	20
26–Jan–98 12:13:02	27–Jan 00:22:43	21785	0.214±0.004	3
03–Feb–98 09:11:10	04–Feb 02:36:39	31150	0.154±0.003	20

[a] Three MECSs on and the source is under the strongback.

Table 4. Period Measurements of RX J0146.9+6121

Observation Date	Period (s)	Error (s)	SATELLITE	Reference
1984 August 27-28	1455	3	EXOSAT	White et al. 1987
1993 February 12-13	1412	4	ROSAT PSPC	Hellier 1994
1994 September 18-19	1407.4	3.0	ASCA	Haberl et al. 1998a
1996 January 21 - February 28	1407.28	0.02	ROSAT HRI	Haberl et al. 1998a
1996 March 28	1407.8	1.3	*Rossi*XTE	This work
1997 January 3	1405.4	0.6	*Beppo*SAX	This work
1997 July 4-10	1404.2	1.2	*Rossi*XTE	Haberl et al. 1998b
1997 August 9	1403.9	1.4	*Beppo*SAX	This work
1998 January 26	1405.6	1.0	*Beppo*SAX	This work
1998 February 3	1401.6	1.4	*Beppo*SAX	This work

spectral and timing results we obtained for 4U 0142+614 are reported elsewhere (Israel et al. 1999a).

After the first observation, one of the three MECS units failed (1997 May 9) and the data of the following pointings were obtained through the remaining two MECS units.

3.1. Spectral analysis

Spectra were extracted from circular regions with radius of $4'$ for both the LECS and MECS instruments and rebinned so as to have $>$30 counts in each energy bin to allow the use of χ^2 statistics. Spectral response matrices appropriate to the particular source off–axis positions were used. These matrices include also a correction for the presence of the strongback used to support the detector entrance window. The background subtraction was performed using source–free regions of each observation at the appropriate off–axis and azimuth angle (to properly take into account the effect of the strongback). We used only MECS counts in the energy range 1.8–10 keV. The background subtracted MECS count rates for each observations are reported in Table 3. All energy bins the count rate of which was consistent with zero were not used in the spectral analysis.

The January 1998 observation, during which RX J0146.9+6121 was observed nearly on-axis, provided the data of best quality. In the limited energy range covered by the LECS and MECS instruments, a power law model provides a satisfactory fit to the spectrum of RX J0146.9+6121. The best fit parameters are photon index of $\alpha = 1.67 \pm 0.1$, N_H = (1.2±0.3) 10^{22} cm^{-2}, corresponding to a flux of 3.1 10^{-11} erg cm^{-2} s^{-1} (2-10 keV, corrected for the absorption). The other three *Beppo*SAX observations gave consistent results in terms of intensity and spectral parameters, to within the large uncertainties related to the calibrations at off-axis angles.

3.2. Timing analysis

The arrival times of the 1–10 keV photons from RX J0146.9+6121 were corrected to the barycenter of the solar system and then used to determine the pulse period. A phase fitting technique was applied in order to better determine the pulse period during each observation; the results are reported in Table 4 (1 σ uncertainties are also given). The light curves in different energy ranges, folded at the best periods, show a broad single–peaked profile with a pulsed fraction of ∼47% which, to within the statistical uncertainties, is energy independent over the 1–10 keV range.

4. Discussion

All the spin period measurements of RX J0146.9+6121 have been collected in Table 4 and are shown in Fig. 5. The first two values, obtained with EXOSAT in 1984 and with ROSAT in 1993, imply a spin-up of at least 1.6×10^{-7} s s^{-1} (equivalent to a spin-up timescale of the order of ∼300 years). Note that this is a lower limit, since we do not know at which time after the 1984 outburst the spin period reached the smaller value measured in recent observations. In contrast, all period measurements obtained after the rediscovery of this source are consistent with small fluctuations around a smaller average spin-up. A linear fit to the 1993-1998 data yields a value of 5.4×10^{-8}s s^{-1}. This behaviour can be interpreted by assuming that the rapid spin-up following the 1984 outburst was due to large angular

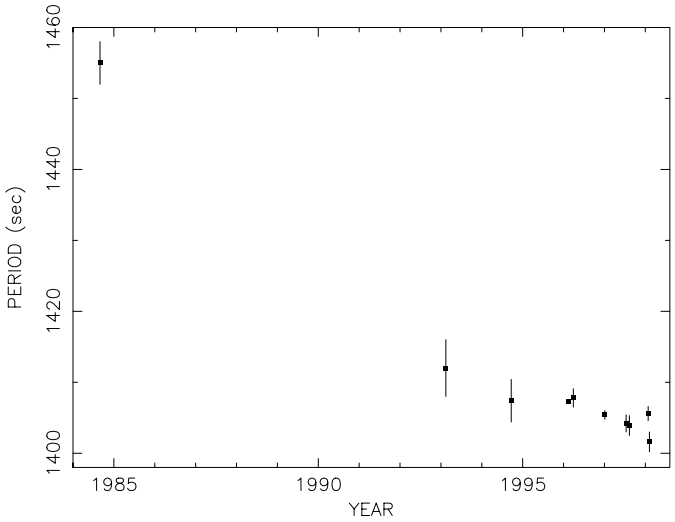

Fig. 5. Pulse period history of RX J0146.9+6121. See Table 4 for details.

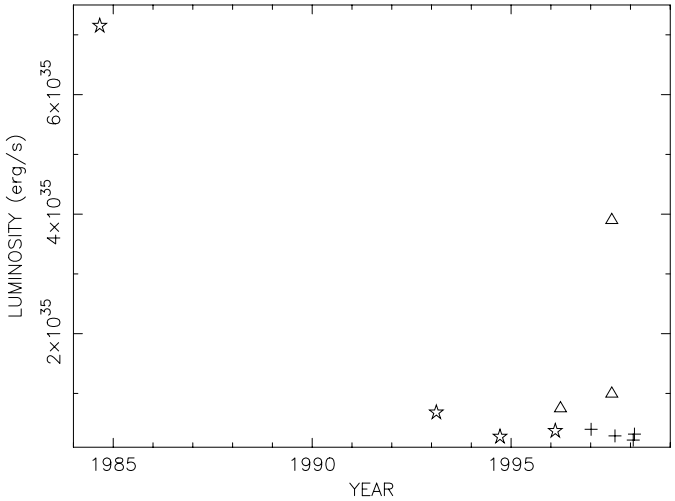

Fig. 6. Luminosity history of RX J0146.9+6121. The luminosities are in the 2–10 keV band and for a distance of 2.5 kpc. Triangles and crosses refer to *Rossi*XTE and *Beppo*SAX observations respectively while stars to data collected by other satellites (EXOSAT, ROSAT and ASCA). Except for the 1984 and July 1997 outbursts, all the flux measurements are consistent with an average luminosity of $\sim 5 \times 10^{34}$ erg s^{-1}.

momentum transfer through an accretion disk in a phase of high accretion rate. Indeed in 1984 RX J0146.9+6121 had a luminosity of $\sim 10^{36}$ erg s^{-1}, while in all subsequent measurements it showed luminosities at least a factor ten smaller. This is illustrated in Fig. 6, where all published flux values are plotted as luminosities for a distance of 2.5 kpc and after the appropriate conversions to the 2-10 keV energy range.

A flux increase of a factor 5 within one week was detected during the *Rossi*XTE observation of July 1997 (Haberl et al. 1998b), indicating the possible start of a new outburst from RX J0146.9+6121. As a consequence one might have expected a corresponding increase in the spin-up. However, our two *Beppo*SAX measurements, obtained respectively one and six months later, did not show any significant variation in the spin period. This might be due to the fact that the July 1997 outburst was smaller (in peak luminosity and possibly in length, see Fig. 6) than the 1984 one.

Though our folded light curve of RX J0146.9+6121 is similar to those reported from previous observations, the better statistics of our data allows to confirm the presence of significant substructure in the pulse profile. Examples of this are the small dip in the main broad peak occurring at phase $\sim$0.6 and the structure in phase interval D, which is visible mostly in the higher energy range. Note that, although RX J0146.9+6121 was brighter during the July 1997 *Rossi*XTE observation reported by Haberl et al. (1998a), on that occasion the source was observed at a large offset angle resulting in a reduced count rate.

The good statistics also permitted, for the first time in this source, to detect variations of the energy spectrum as a function of the pulse period phase.

We finally note that, contrary to previous reports we do not find any evidence for a spectral cut-off at low energy. A spectral cut-off at $\sim$4 keV was obtained by a combined spectral fit of non simultaneous *Rossi*XTE and ASCA data (Haberl et al. 1998b) and interpreted as possible evidence for a relatively weak magnetic field of the order of a few 10^{11} G. Our results indicate a cut-off value in the range usually observed in X–ray pulsars.

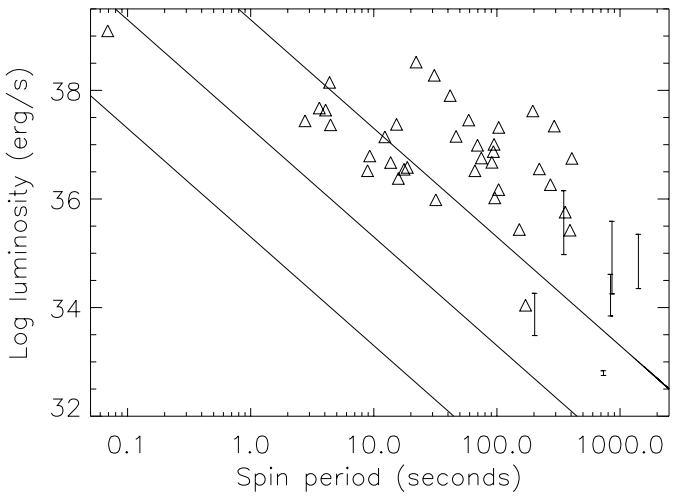

Fig. 7. Correlation between X-ray luminosity (in the range 2-10 keV) and spin period of all the Be X-ray pulsar systems. For transient sources (triangles) only maximum luminosities are plotted. The three lines correspond to the centrifugal equilibrium (White et al. 1995) for different values of the magnetic field (from left to right: 10^{11}, 10^{12}, 10^{13} G).

Until recently RX J0146.9+6121 and X Persei had extreme properties among Be X-ray pulsars, by virtue of their long spin period and relatively low luminosity. New X–ray and optical observations led to the discovery of a few other systems with similar characteristics: RX J0440.9+4431, RX J1037.5–564 (Reig & Roche 1999), 1WGA J1958.2+3232 (Israel et al. 1998), and possibly 1SAX J0103.2–7209 (Israel et al. 1999b).

These long period X-ray pulsating sources are characterized by relatively low and steady luminosities, in contrast with the brighter systems the discovery of which has been favoured in the past during their strong outbutsts. This is illustrated in Fig. 7, which shows the luminosity versus pulse period of the 44 X–ray pulsars with Be companions currently known. For RX J0146.9+6121 and the other similar sources mentioned above, we have indicated the observed range of luminosity values. For the other systems we have reported the maximum observed luminosity, since in most cases only upper limits or very uncertain values exist for their quiescent fluxes. Note that fast spinning, magnetized neutron stars are not visible at low luminosities, owing to the action of the centrifugal barrier in preventing accretion onto the neutron star surface (Stella et al. 1986). On the other hand, neutron stars with spin periods longer than a few hundreds seconds can easily display pulsed emission at low accretion rates. Future, more sensitive observations will further increase this sample that probably forms the bulk of the Be/neutron star binaries.

References

Boella G., Butler R.C., Perola G.C., et al., 1997a, A&AS 122, 299
Boella G., Chiappetti L., Conti G., et al., 1997b, A&AS 122, 327
Bradt H.V., Rothschild R.E., Swank J.H., 1993, A&AS 97, 355
Coe M.J., Everall C., Norton A.J., et al., 1993, MNRAS 261, 599
Dove J.B., Wilms J., Nowak M.A., et al., 1998, MNRAS 298, 729
Haberl F., Angelini L., Motch C., White N.E., 1998a, A&A 330, 189
Haberl F., Angelini L., Motch C. 1998b, A&A 335, 587
Hellier C., 1994, MNRAS 271, L21
Israel G.L., Mereghetti S., Stella L., 1994, ApJ 433, L25
Israel G.L., Stella L., Campana S., et al., 1998, IAU Circ. 6999
Israel G.L., Oosterbroek T., Angelini L., et al., 1999a, A&A 346, 929
Israel G.L., Covino S., Polcaro V.F., Stella L., 1999b, A&A 345, L1
Jahoda J., Swank J.H., Giles A.B., et al., 1996, SPIE 2808, 59
Koyama K., Awaki H., Kunieda H., et al., 1989, Nat 339, 603
Mereghetti S., Stella L., De Nile F., 1993, A&A 278, L23
Motch C., Belloni T., Buckley D., et al., 1991, A&A 246, L24
Motch C., Haberl F., Dennerl K., Pakull M., Janot-Pacheco E., 1997, A&A 323, 853
Parmar A.N., Martin D.D.E., Bavdaz M., et al., 1997, A&AS 122, 309
Reig P., Roche P., 1999, MNRAS 306, 100
Slettebak A., 1985, ApJ Suppl 59, 769
Stella L., White N.E., Rosner R., 1986, ApJ 308, 669
Strohmayer T., Jahoda K., 1998, Field of View of the PCA. http://lheawww.gsfc.nasa.gov/users/keith/fieldofview/collimator.html
Tapia M., Costero R., Echevarra J., Roth M., 1991, MNRAS 253, 649
White N.E., Nagase F., Parmar A.N.. 1995, In: Lewin W.H.G., van Paradijs J., van den Heuvel E.P.J. (eds.) X–ray Binaries. Cambridge Cambridge Univ. Press, p. 1
White N.E., Mason K.O., Giommi P., et al., 1987, MNRAS 226, 645
White N.E., Angelini L., Ebisawa K., Tanaka Y., Ghosh P., 1996, ApJ 463, L83
Yamauchi S., Koyama K., 1993, ApJ 404, 620